

# 3D simulation of air velocity effect on the flow water level in horizontal confined channel

Hella Adouni<sup>#1</sup>, Yoldoss Chouari<sup>#2</sup>, Wassim Kriaa<sup>#3</sup>, Hatem Mhiri<sup>#4</sup>, Philippe Bournot<sup>\*5</sup>

<sup>#</sup>UTTPI, National Engineering School of Monastir, Monastir, Tunisia

<sup>1</sup>hella.adouni2@gmail.com

<sup>\*</sup>IUSTI, UMR CNRS 6595,5 rue Enrico Fermi, Technopole de Château-Gombert

<sup>5</sup>philippebournot@yahoo.fr

**Abstract**— The flows often occurring in sewerage networks are marked by the presence of pressurized air above the treated water. The pressurized air may have a negative effect on the sanitation infrastructure causing serious accidents, such as geyser phenomena, leaks, violent expulsion of the manhole cover, etc. This explains the importance of the study of two-phase flows in sewer networks. The aim of our work is to develop a numerical model that can simulate two-phase flows in confined channels and then to study the effect of air velocity on flow dynamics. The geometric modeling of the study area was performed using the "Gambit" software. The numerical simulation of the air/water flow is carried out on the Fluent software. To predict the air/water interface, the VOF (Volume Of Fluid) model has been adapted. The turbulence model chosen is the RNG K-  $\epsilon$  Model. A comparison between the velocity profiles and the experimental results obtained was carried out in order to validate the model. Several meshes were tested. The results showed that to gain in computation time and accuracy, the mesh chosen is the one consisting of 1,314,000 cells, from which the results no longer vary. Therefore, the model developed is perfectly suited to our case study and enables us to precisely predict the behavior of a two-phase flow in a closed channel.

**Keywords**— two phase flow, air-water internal flow, air velocity effect, interfacial behaviour, VOF

## I. INTRODUCTION

Two-phase flows in pipes, also called internal flows, are generally characterized by an interface that constitutes the place where energy is transmitted between the two phases. This type of flow is found in sewerage networks where it is essential to understand the mechanisms of these exchanges, quantify them precisely and monitor their evolution in order to avoid the hydraulic failures they can generate such as manhole overflows initiating flooding, the phenomenon of water hammer, pipe breakage, leaks, geyser phenomena, violent expulsion of the manhole cover, etc [1], [2].

This is a topical research subject since accidents that occur due to misunderstanding of the internal flow are serious. The studies carried out on urban sewerage networks exploit practically 3 sections that start from pipe's initial size dimensioning, passing through the internal behaviour of the flow up to the evacuation of pollutants in the ejection points (sea, river...). This paper focuses on understanding the

air/water interaction that is the driving force behind the transition from gravity flow to forced flow.

In this context, Hamam and McCorquodale [3] conducted experimental tests on a two-phase gravity and confined flow that suddenly turns into a forced flow. The size of the pipe, its shape, speed, flow rate, Froude number, relative depth of flow, slope of the pipe, aeration arrangement... are among the factors that cause this transition. Their tests highlighted the high pressures that generally occurs with transient flows and described the transition to a forced flow in three steps, which are the formation of a surge, the formation of instabilities, and the transition to a forced flow. This transition to forced flow is accompanied by phases of air entrapment that have been the subject of several studies [3], [4] due to their significant effect on the pipes. Initial and boundary conditions are among the factors that stimulate the creation of air pockets in wastewater systems. The results of Hamam and McCorquodale [3] showed that when the ratio between water velocity phase and air velocity reaches a certain limit

$V = 6.46$  m/s given by Kelvin\_Hemholtz, a large air pocket is formed. The air pockets will be expelled at the evacuation points generating pressure peaks similar to "waterhammer", thus disrupting the water flow. In this perspective, the results given by Li and McCorquodale [6] showed that these pressure peaks are caused either by the change in flow conditions (sudden closure of a valve) or by the evacuation of air bubbles during rapid pipe filling. Air enters the pipes and can be trapped during rapid filling [7]. This filling causes the compression or evacuation of air pockets, resulting in significant pressure variations. Insufficient ventilation is also one of the factors that stimulate air pockets creation. Flow conditions are becoming more complex when it comes to lack of aeration [8]. Indeed, an unsuitable ventilation system leads to the creation of large air bubbles in the flow [9]. When the capacity of the air flow fails to move the air bubbles in the channel, they will accumulate forming a large bubble that will generate pressure on the water leading to the blockage of the pipe in some cases [10]. This usually happens for large slope variations [11]. Thus, in order to avoid the accumulation of air pockets, it is essential to know the regime of these flows and particularly the boundary conditions that make the transition from one regime to another [12]. Several studies [13], [14] have turned to the numerical approach for

characterizing flow regimes and studying their behaviour under different boundary conditions. F.Vasquez [13] reproduced the behaviour of bubble, laminate and pocket flow for the determination of pressure drop and liquid retention to demonstrate the applicability of CFD in solving two-phase fluid problems in horizontal pipes. The results showed that CFD is desirable for predicting dispersed and stratified flows with a margin of error of 20%. Sandra De Schepper [14] reproduced all possible two-phase air-water flow regimes in a horizontal pipe while validating her results with those of Baker (1954), in order to confirm the credibility of CFD codes in terms of solving two-phase fluid problems. To do this, the VOF model was used in combination with the PLIC interface reconstruction method. In addition, compared to the extensive studies available on two-phase flows in small diameters ( $D < 50$  mm), little researches has been conducted on two-phase horizontal flows in large diameters although the actual size of pipes in engineering systems may be relatively large, compared to that used in an experimental environment [15].

However, after a literature review, it was found that there is a considerable lack of literature regarding the effect of air velocity on water in a horizontal confined channel. Nevertheless, it is an essential parameter for understanding and controlling the behaviour of internal flow. We are therefore looking to develop a three-dimensional numerical model able to simulate an air water two phase flow in horizontal confined channel with large Diameter ( $D = 100$  mm) in the first place and then to study the effect of air velocity on water level.

## II. MATHEMATICAL FORMULATION

### 1) Assumptions

The modelling assumptions used for the two phase flow simulation are as follows.

- The two-phase flow is composed of two fluids (air and water) that are incompressible and in turbulent conditions
- The two fluids considered are Newtonian and immiscible
- The flow is unsteady and isothermal
- The effect of surface tension is taken into account

The proposed methodology for the numerical simulation of air/water flow in the channel under consideration is developed on the Fluent software; a commercially licensed software allowing 2D and 3D simulations to be performed in fluid mechanics. A 3D model is adopted to take into consideration the depth of the channel and to get closer to the real case. The dimensions considered in this work correspond to those of the hydraulic canal of the laboratory located at the IUSTI of the University of Aix Marseille; rectangular and confined canal 5m length, 0.075m wide and 0.15m deep (Fig.1) where the experimental part was carried out.



Fig. 1 Domain geometry modeled and meshed

### 2) Governing equations [16]

The equations that govern the flow are the Navier Stokes equations which are the mass conservation equation (1), and the conservation of momentum (2).

$$\frac{\partial \rho}{\partial t} + \frac{\partial \rho u_i}{\partial x_i} = 0 ; i=1, 2, 3 \quad (1)$$

$$\frac{\partial \rho u_i}{\partial t} + \frac{\partial \rho u_i u_j}{\partial x_j} = - \frac{\partial P}{\partial x_i} + \frac{\partial \tau_{ij}}{\partial x_j} + \rho f_i \quad (2)$$

- $\rho$  : Fluid density
- $P$ : Static pressure
- $U$ : Fluid velocity
- $f_i$ : External body forces
- $\tau_{ij}$  : Stress tensor

$$\tau_{ij} = \mu \left( \frac{\partial u_i}{\partial x_j} + \frac{\partial u_j}{\partial x_i} \right) - \frac{2}{3} \mu \delta_{ij} \frac{\partial u_k}{\partial x_k} \quad (3)$$

- $\mu$  : Viscosity
- $\delta$  : Kronecker symbol

Flow resolution requires turbulence model. In this case study three turbulence model are tested:

- The Standard K-  $\epsilon$  Model
- The RNG K-  $\epsilon$  Model
- The Realizable K-  $\epsilon$  Model

To predict the air-water interface, the VOF model was chosen. The tracking of the air-water interface is achieved by the solution of a continuity equation for the volume fraction of each phase. For the qth phase, this equation has the following form:

$$\frac{1}{\rho_q} \left[ \frac{\partial}{\partial t} (\alpha_q \rho_q) + \nabla \cdot (\alpha_q \rho_q \vec{u}_q) \right] = 0 \quad (4)$$

Where the qth fluid's volume fraction in the cell is denoted as  $\alpha_q$ .

The volume fraction equation will not be solved for the primary phase; the primary-phase volume fraction will be computed based on the following constraint:

$$\sum_{q=1}^n \alpha_q = 1 \quad (5)$$

The volume-fraction-averaged density takes on the following form:

$$\rho = \sum \alpha_q \rho_q \quad (6)$$

All other properties (e.g., viscosity) are calculated in the same way.

### 3) Boundary conditions

Boundary conditions are necessary to ensure the stability and accuracy of the simulation results. The velocity inlet condition is imposed at the air inlet and water inlet. At the outlet, the "Outflow" condition is imposed as shown in Fig.2. The boundary conditions are summarized in Table I.

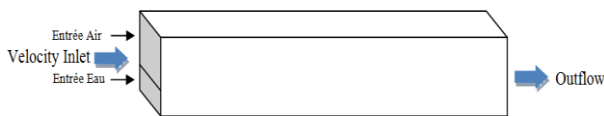


Fig. 2 Boundary condition for air water flow through the channel

Table I  
Boundary conditions

Boundary conditions		H <sub>water</sub>		Formulation
		Velocity (m/s)	Turbulence	
Air inlet	« Velocity inlet »	3.48	K =0.0698 ε =0.4720	U <sub>init</sub>
Water inlet	« Velocity inlet »	0.47	K=0.0015 ε =0.0031	U <sub>init</sub>
Channel's upper side	« No Slip »	---	---	U=V=W=0
Channel's lower side	« No Slip »	---	---	U=V=W=0
Outlet	« Outflow »	---	---	$\frac{\partial \phi}{\partial x} = 0$

Φ : Variable (U, V, W,...) according to spatial coordinates.

The turbulent kinetic energy k is estimated from the turbulent intensity:

$$K = \frac{3}{2} (u_{avg} I)^2 \quad (7)$$

Where  $u_{avg}$  is the mean flow velocity and I is the turbulence intensity.

$$I = 0.16 (Re_{D_H})^{-1/8} \quad (8)$$

Reynolds number is calculated as follows:

$$Re = \frac{\rho D_H U}{\mu} \quad (9)$$

Where  $D_H$  is the hydraulic Diameter.

Turbulent dissipation rate is obtained from the following relationship:

$$\epsilon = C_u \frac{3/4 k^{3/2}}{l} \quad (10)$$

Where  $C_u$  is an empirical constant specified in the turbulence model (approximately 0.09) and l is the turbulence length scale.

The turbulence length scale l is a physical quantity related to the size of the large eddies that contain the energy in turbulent flows.

$$l = 0.07 D_h \quad (11)$$

### III. NUMERICAL METHOD

Gambit and Fluent, two commercially licensed software packages, were used to perform 3D simulations in fluid mechanics ranging from mesh construction with Gambit to solving Navier Stokes equations and post processing with Fluent. The specification of the mesh size depends on the complexity of the geometry. Since the geometry considered is rectangular, a hexahedral mesh grid was chosen. The number of meshes at the four walls at the inlet, as well as at the interface, is increased to ensure high resolution and accuracy during flow transitions (Fig. 3). All numerical simulations were performed using the second order upwind scheme. The "PISO" method was used to calculate the Pressure/Speed coupling. For all cases studied in this paper, a transient simulation with a time step of 0.0001 was identified.

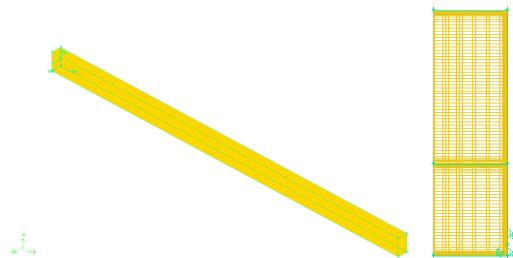


Fig. 3 Domain geometry modeled and meshed

In this work, we plan to carry out 10 numerical simulations studying the behavior of a two-phase air/water flow within a horizontal channel confined under variations in air velocity as listed in Table II.

### IV. RESULTS AND DISCUSSION

#### 1) Validation Mesh sensitivity analysis

In order to study the sensitivity of the results to the mesh size, three different mesh sizes were checked for a water level  $H_L = 0.032m$ : M1=930 000 cells; M2=1 314 000 cells; M3=1 800 000 cells.

The respective water and air velocities of mesh sensitivity test were:  $V_{water} = 0.47 m/s$  and  $V_{air} = 3.2 m/s$ . The simulation of the different meshes is performed using the standard k-ε turbulence model. As seen in Fig. 4, there is no significant difference between the results of the simulations performed using the 1,314,000 cells and the 1,800,000 cells. Thus, to save calculation time, the mesh size chosen is that consisting of 1,314,000 cells.

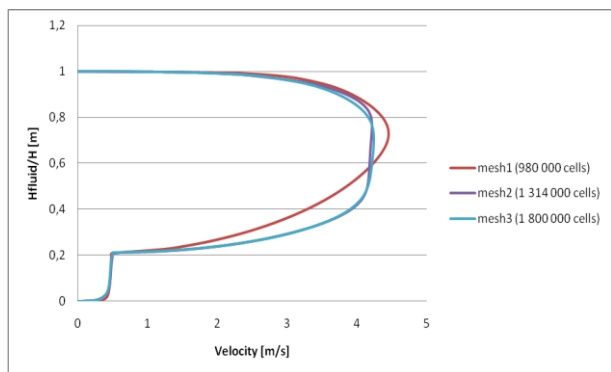


Fig. 4 Mesh sensitivity analysis

2) Turbulence model validation :

In order to choose the best turbulence model, simulations were performed with the first order models K- $\epsilon$  Standard, K- $\epsilon$  RNG and K- $\epsilon$  Realisable. The K- $\epsilon$  RNG model is considered sufficient to predict flow quantities as shown in Fig. 5. The RNG k- $\epsilon$  model is similar in form to the standard k- $\epsilon$  model, but includes an additional term in its  $\epsilon$  equation that significantly improves the accuracy for rapidly strained flows. Since, this work is based on the study of flow pattern under several air velocities; it is more suitable to use the RNG K- $\epsilon$  model.

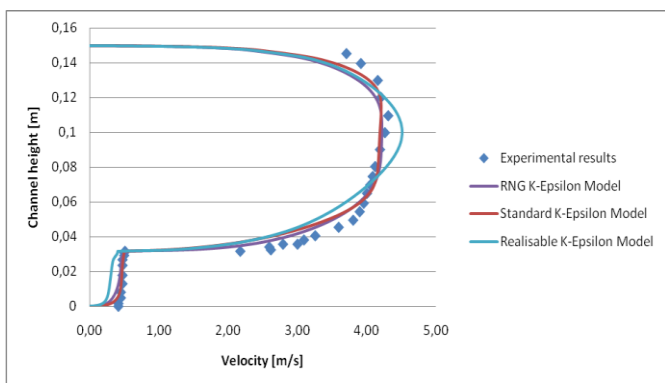


Fig. 5 Turbulence model validation

3) The effect of air velocity on the water level:

Ten cases of air-water volumes fractions have been investigated as shown in Table II. In all cases, the liquid superficial velocity was constant at  $V_{water} = 0.16$  m/s and introduced from the bottom region with a liquid level  $H_L = 0.055$ m.

Table II The superficial velocities for the simulation cases

Air-Water cases	Water superficial velocity (m/s)	Air superficial velocity (m/s)
Case 1	0.16	0.5
Case 2		1
Case 3		2
Case 4		1.5
Case 5		3
Case 6		5
Case 7		6
Case 8		7
Case 9		8
Case 10		9

Fig. 6 describes the effect of the superficial air velocity on the water level in the channel.

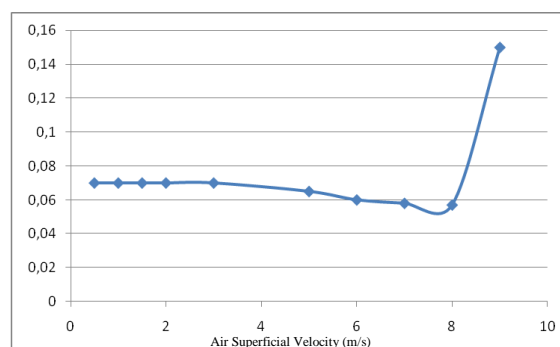


Fig. 6 The effect of the superficial air velocity on the water level

Under  $V_{air}^S = 3$ m/s, a stratified smooth flow is observed. The air is at the top of the channel and the water is at the bottom (Fig. 8.a). Liquid level  $H_L$  is independent from the superficial air velocity. Above  $V_{air}^S = 3$ m/s, the liquid level start showing a light decrease as the superficial air velocity increases. Periodic 2D waves with small amplitude appears at the interface, and the water level is getting slightly lower (Fig. 8.b). The interfacial behaviour is regular and dependent to gas flow rate. As  $V_g$  increases, it creates drag forces that reduces the liquid level and increases the area occupied by the air phase as shown in velocity profiles in Fig. 7. It is also noticed that the maximum water velocity is near the interface whereas the maximum air velocity is shifted closer to the upper side of the channel.

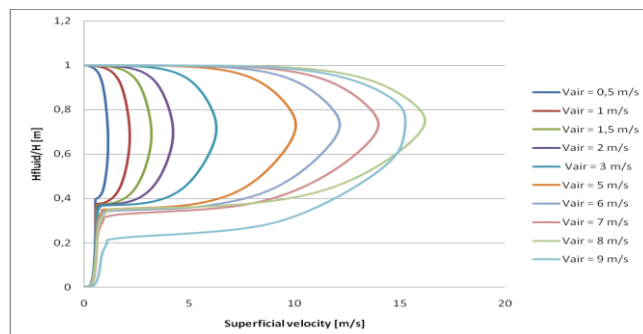


Fig. 7 Longitudinal velocity profiles for  $x = 1.5$ m

Starting from a superficial air velocity  $V_{air}^S = 9\text{m/s}$  the water level begins to grow. As the gas passes over the wave, an upward wave force is raising the wave until it reaches the top wall of the channel. Significant interfacial instabilities are observed (Fig. 8.c). This interfacial behaviour forms into the slug shape.

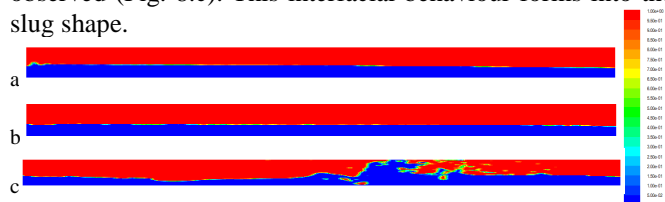


Fig. 8 Contours of density for water-air flow: (a) smooth interface (b) wavy interface with decrease in water level (c) high instability interface

The speed of this slug creation and its location from the inlet is dependant to the gas velocity. Indeed, as  $V_g$  increases the slug is closer to the inlet and faster as shown in Fig. 9 and Fig. 10.

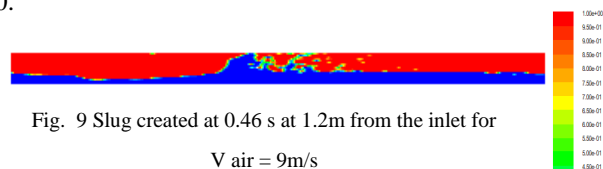


Fig. 9 Slug created at 0.46 s at 1.2m from the inlet for

$V_{air} = 9\text{m/s}$

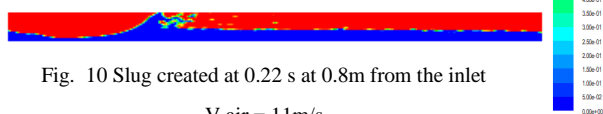


Fig. 10 Slug created at 0.22 s at 0.8m from the inlet

$V_{air} = 11\text{m/s}$

## V. CONCLUSIONS

Consideration was given in the present study to the effect of air velocity on a two phased flow into a confined horizontal channel with large diameter. Behavior of the flow was effectively predicted by the 3D VOF model with RNG K- $\epsilon$  turbulence model.

The conclusions reached from this study are recapitulated in the following key notes:

- Under constant superficial water velocity  $V_{water}^S = 0.16\text{ m/s}$ , the flow shows different behavior

according to gas velocity raise: Going from stratified smooth flow with flat interface, passing through 2D waves with regular form, reaching significant instabilities where waves touches the upper wall of the channel;

- Liquid level decreases as the gas level increases;
- The higher the gas velocity, the faster the wave formation is and the closer to the inlet.

## REFERENCES

- [1] Pozos-Estrada, O., et al. "Failure of a drainage tunnel caused by an entrapped air pocket." *Urban Water J.*, 2015
- [2] Vasconcelos, J. G., and Leite, G. M. "Pressure surges following sudden air pocket entrapment in storm-water tunnels." *J. Hydraul. Eng.*, 2012
- [3] Hamam, M. A., and McCorquodale, J. A, "Transient conditions in the transition from gravity to surcharged sewer flow", 1982
- [4] Zhou, F., Hicks, F., and Steffler, P, "Analysis of effect of air pocket on hydraulic failure of urban drainage infrastructure." 2004
- [5] Vasconcelos, J. G., Klaver, P. R., and Lautenbach, D. J, "Flow regime transition simulation incorporating entrapped air pocket effects." 2015
- [6] Li, J., and McCorquodale, A, "Modeling mixed flow in storm sewers." *J. Hydraul. Eng.*, 1999.
- [7] Lauchlan, C. S., Escarameia, M., May, R. W. P., Burrows, R., and Gahan, C. "Air in pipelines: A literature review", HR Wallingford, Oxfordshire, U.K., 2005
- [8] Zhou, F., Hicks, F. E., and Steffler, P. M. (2002a). "Observations of air-water interaction in a rapidly filling horizontal pipe." *J. Hydraul. Eng.*, 2002
- [9] Vasconcelos, J. G., and Wright, S. J. "Mechanisms for air pocket entrapment in stormwater storage tunnels." *Proc., World Environmental and Water Resources Congress 2006*
- [10] Granata, F., de Marinis, G., and Gargano, R. "Air-water flows in circular drop manholes." *Urban Water J.*, 2015
- [11] Lubbers, C. L., and Clemens, F. H. L. R. (2005b). "Capacity reduction caused by air intake at wastewater pumping stations." *Proc., 3rd Int. Conf. on Water and Wastewater Pumping Stations*, P. May, ed., BHR Group, U.K., 2005
- [12] Christophe Conan, « étude expérimentale et modélisation des écoulements liquide-liquide en conduite horizontale », 2007
- [13] F. Vásquez, M. Stanko, A. Vásquez, J. De Andrade & M. Asuaje "Air-water: two phase flow behavior in a horizontal pipe using computational fluids dynamics (CFD)", 2012
- [14] Sandra C.K. De Schepper, Geraldine J. Heynderickx, Guy B. Marin "CFD modeling of all gas-liquid and vapor-liquid flow regimes predicted by the Baker chart", 2007
- [15] Ran Kong "Characterization of horizontal air-water two phase-flow", 2015
- [16] FLUENT 6.2 User's Guide, 2005